Crystal-field interactions and spin reorientation in $(Er_{1-x}Dy_x)_2Fe_{14}B$

H. R. Rechenberg* and J. P. Sanchez
Centre de Recherches Nucléaires, Boîte Postale 67037, Strasbourg Cédex, France

P. L'Héritier and R. Fruchart
Ecole Nationale Supérieure de Physiciens de Grenoble, 38402 Saint Martin d'Hères, France
(Received 16 December 1986)

Spin reorientation in $(Er_{1-x}Dy_x)_2Fe_{14}B$ alloys has been investigated by means of ^{57}Fe Mössbauer spectroscopy on magnetically aligned samples. For $0<x<0.5$, the magnetization direction is found to change continuously from the basal plane to the tetragonal c axis with increasing temperature. Reorientation temperatures decrease with increasing Dy concentration, as expected from competition between the uniaxial anisotropy of Dy and the basal anisotropy of Er in the $R_2Fe_{14}B$ (R a rare-earth atom) structure. Data are quantitatively interpreted with a model incorporating crystal-field and exchange interactions as well as Fe-sublattice and R dipolar anisotropies. The stability range of the basal-plane magnetization extends up to $x_c \simeq 0.5$ at low temperatures, while the model predicts $x_c = 0.26$ if only $B_2^0O_2^0$ and $B_2^2O_2^2$ terms are considered; inclusions of $B_4^0O_4^0$ and $B_6^0O_6^0$ terms provide a satisfactory fit to our T_r versus x data.

I. INTRODUCTION

A great deal of experimental and theoretical effort has been devoted in the last three years to the tetragonal $R_2Fe_{14}B$ (R denotes a rare-earth atom) intermetallic compounds.[1] Soon after the discovery of the new $Nd_2Fe_{14}B$ phase,[2,3] it was recognized that crystalline electric fields (CEF's) acting on the R ions are the primary cause of the high magnetic anisotropies found in most of these compounds. From x-ray diffraction and magnetization measurements on oriented powder samples, it was inferred[4] that the easy magnetization direction is parallel to the c axis for R = Pr, Nd, Tb, Dy, and Ho, and perpendicular to the c axis for R = Sm, Er, and Tm. Since these two groups of rare-earth metals are characterized by second-order Stevens coefficients (α_J) of opposite signs, it was concluded that the gross features of magnetic anisotropy (i.e., easy-axis or easy-plane magnetization) are determined by the second-order CEF terms. Similar correlations had been previously observed in other rare-earth–transition-metal compounds.[5] It seems, however, that the gradual spin canting occurring below 150 K for $Nd_2Fe_{14}B$ (Ref. 6) and below 58 K for $Ho_2Fe_{14}B$ (Ref. 7) cannot be accounted for without inclusion of higher-order terms in the CEF Hamiltonian.[8] When R is a nonmagnetic (Y, La, Ce, Lu) or S-state (Gd) ion, the easy magnetization direction is always parallel to the c axis, indicating that the Fe sublattice has a uniaxial magnetic anisotropy of its own. The Fe anisotropy energy, such as deduced from $Y_2Fe_{14}B$ or $Gd_2Fe_{14}B$ data,[7] has a peculiar temperature dependence, showing a maximum at $T \simeq 0.6T_C$. In those compounds for which R has basal anisotropy, therefore, competition between both terms may lead to a spin reorientation from the basal plane to the c axis with increasing temperature. Such transitions have indeed been observed[9–12] for R = Er, Tm, and Yb.

By partial substitution of, e.g., Er by another rare-earth element, one can modify the average R anisotropy and thereby change the reorientation temperature. The point of interest here is that, due to the structural similarity of the $R_2Fe_{14}B$ compounds, if a set of CEF parameters is known for a given R, the CEF parameters for a substituent R' can be obtained by appropriate scaling, thus allowing the effect of substitutions to be predicted without introducing new, independent parameters. In this manner, a study of spin reorientation temperatures as a function of x in $(R_{1-x}R'_x)_2Fe_{14}B$ seems promising as a means of testing microscopic models for the CEF and exchange interactions in these compounds.

The spin reorientation in $(Er_{1-x}Gd_x)_2Fe_{14}B$ alloys has been recently investigated in our group, by means of Mössbauer spectroscopy.[13] T_r versus x data were quantitatively explained in terms of a Hamiltonian which included second-order CEF terms and the R-Fe exchange interaction, plus a uniaxial anisotropy due to the Fe sublattice. Since the S-state Gd ion does not contribute to the CEF anisotropy, its effect is to gradually reduce the spin reorientation temperature.

In this work we report on an investigation of the spin reorientation in the $(Er_{1-x}Dy_x)_2Fe_{14}B$ system. In contrast to Gd, Dy has a strong anisotropy favoring the c axis; it thus actively competes with the Er basal anisotropy, and a more rapid decrease of T_r as a function of x is expected. Our data confirm this expectation and show quantitative agreement with the T_r versus x predictions of a second-order CEF model, but only for small x; for higher Dy concentrations—i.e., for lower T_r—our results clearly demonstrate the necessity of taking fourth-order and sixth-order terms into consideration.

Very recently, Niarchos and Simopoulos[14] have reported a similar study on the same alloy system, with results in essential agreement with ours. No quantitative analysis was made, however.

II. EXPERIMENTAL PROCEDURES

The pseudoternary alloys were prepared from near-stoichiometric amounts of high-purity elements by cold crucible melting, followed by vacuum annealing at 900 °C during two weeks. Quality checks were provided by powder x-ray diffraction, ^{57}Fe Mössbauer spectroscopy, and magnetization measurements. Mössbauer spectra were taken at room temperature and were fitted with six magnetically split subspectra, including quadrupole interactions as a perturbation, whose relative intensities were fixed at the theoretical populations of the six Fe sites.[15] α-Fe and $R_{1+\epsilon}Fe_4B_4$ (Ref. 16) were systematically present as impurity phases (at most 6%). Lattice constants (a,c), ferromagnetic ordering temperatures (T_C), and average Fe hyperfine field $(\langle H_{\text{eff}}\rangle)$ for all samples are shown in Table I. All these quantities vary smoothly with Dy concentration, confirming that our $(Er_{1-x}Dy_x)_2Fe_{14}B$ samples were homogeneous solid solutions.

The spin reorientation was detected by observing the relative intensity change of the $\Delta m = 0$ Mössbauer resonance lines in magnetically aligned samples. This method relies on the fact that, for a magnetically split ^{57}Fe spectrum, the intensities of the six lines are (ideally) in the ratios $3:Z(\alpha):1:1:Z(\alpha):3$, where α is the angle between the γ-ray wave vector and the hyperfine field direction, and $Z(\alpha)=4\sin^2\alpha/(1+\cos^2\alpha)$. Thus, for an absorber whose spins are initially aligned parallel to the γ-ray direction, a 90° spin reorientation will manifest itself as a $Z(\alpha)$ change from 0 to 4.

Aligned absorbers containing 10 mg Fe/cm^2 were prepared by dispersing finely powdered material in molten paraffin at 60 °C, and letting the mixture solidify by cooling while keeping it in the magnetic field ($\simeq$0.2 T) provided by two small permanent magnets. The degree of alignment thus achieved, though not perfect, was sufficiently high for the purpose of this investigation.

Mössbauer measurements were carried out with a ^{57}Co-Rh source, driven (linearly or sinusoidally) in synchronization with a multichannel analyzer working in the time mode. A liquid-nitrogen flow cryostat was used for measurements above 77 K and a helium-bath cryostat provided with a temperature controller was used between 4.2 and 77 K.

III. RESULTS

The expected line-intensity relationship for a sample in both the easy-axis ($T > T_r$) and easy-plane ($T < T_r$) magnetization states are illustrated by the spectra in Fig. 1. Even at room temperature, all spectra exhibited a residual absorption corresponding to the $\Delta m = 0$ lines, which must be attributed to incomplete magnetic alignment.

The limited spectral resolution connected to the presence of many distinct crystallographic sites, the magnetic inequivalence of crystallographic equivalent sites when the magnetization is not in the c direction, as well as the poorer statistics for aligned absorbers, make a complete analysis of the spectra difficult and unreliable. Therefore, visual inspection without recurring to rigorous fits is considered sufficient in order to conclude on the essential features of the reorientation effects under consideration.

TABLE I. Lattice constants (a,c), Curie temperatures (T_C), and average hyperfine field on ^{57}Fe at 295 K $(\langle H_{\text{eff}}\rangle)$ for $(Er_{1-x}Dy_x)_2Fe_{14}B$ samples used in this work.

X	a (Å)	c (Å)	T_C (K)	$\langle H_{\text{eff}}\rangle$ (T)
0.1	8.735(1)	11.959(1)	588(3)	28.3(3)
0.2	8.740(1)	11.963(1)	568(3)	28.6(3)
0.3	8.743(1)	11.966(1)	570(3)	28.9(3)
0.4	8.747(1)	11.971(1)	571(3)	29.1(3)
0.5	8.748(1)	11.983(1)	577(3)	29.6(3)
0.6	8.751(1)	11.991(1)	580(3)	29.7(3)
0.8	8.754(1)	11.998(1)	588(3)	30.0(3)

Increase of the $\Delta m = 0$ intensity was observed in all cases to occur over a finite temperature range, which increased with Dy concentration. The same kind of behavior was reported in Ref. 14. In contrast, spin reorientations in $Er_2Fe_{14}B$ (Refs. 9 and 10) and in $(Er_{1-x}Gd_x)_2Fe_{14}B$ (Ref. 13) take place over temperature ranges never exceeding 10 K. As will be shown below, experimental and theoretical arguments give support to a gradual spin-reorientation process in $(Er_{1-x}Dy_x)_2Fe_{14}B$.

Figure 2 shows the concentration dependence of the spin-reorientation temperature, as inferred from our Mössbauer measurements. Error bars indicate the temperature interval over which line intensities were observed to change. For $x \geq 0.5$, no reorientation was detected down to 4.2 K. Data from Ref. 14 are reproduced in Fig. 2 for comparison. There is agreement for $x \leq 0.25$, but for higher concentrations our T_r data have a smoother x

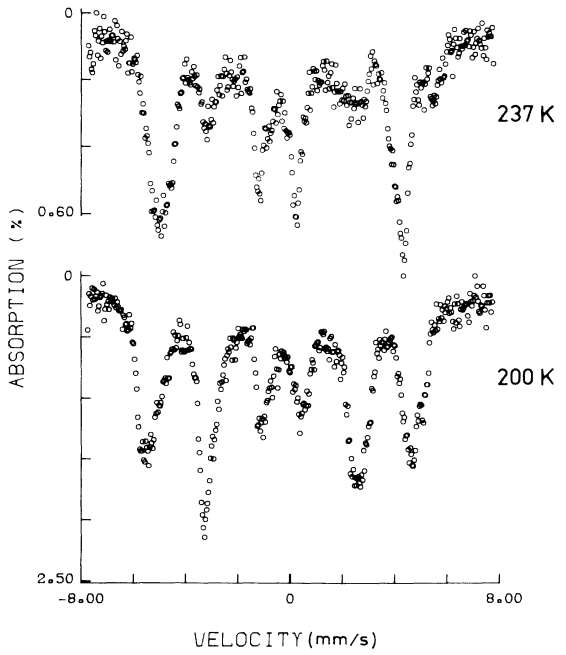

FIG. 1. Mössbauer spectra of magnetically aligned $(Er_{0.9}Dy_{0.1})_2Fe_{14}B$ at temperatures above and below the spin reorientation.

dependence. The largest discrepancy between our data and those of Ref. 14 concerns the region of the critical concentration x_c, above which magnetization is parallel to the c axis down to 4.2 K or below.

IV. DISCUSSION

The rare-earth contribution to the magnetic anisotropy will be described in terms of a single-ion Hamiltonian[17] comprising the CEF interaction with the $4f$ electrons and the exchange interaction

$$\mathcal{H}=\mathcal{H}_{\rm CEF}+\mathcal{H}_{\rm ex} , \tag{1}$$

where

$$\mathcal{H}_{\rm CEF}=B_2^0O_2^0+B_2^2O_2^2 , \tag{2}$$

expressed in terms of Stevens operators,[18] is truncated to second order as a first approximation, and

$$\mathcal{H}_{\rm ex}=-g_J\mu_B H_{\rm mol}\mathbf{J}\cdot\mathbf{n} \tag{3}$$

is expressed in terms of an isotropic molecular field.

For a given set of B_n^m and $H_{\rm mol}$ parameters and a given magnetization direction $\mathbf{n}$, the eigenvalues of (1) are found by numerical diagonalization within the ground-state J manifold. The free energy per rare-earth ion is then calculated according to $F_R=-kT\ln Z$, where Z is the partition function. In the tetragonal $R_2Fe_{14}B$ structure, the R ions occupy two nonequivalent crystallographic sites, $4f$ and $4g$.[19–21] It will be assumed that Er and Dy ions in $(Er_{1-x}Dy_x)_2Fe_{14}B$ are randomly distributed over the two sites, so that the averaged R magnetocrystalline free energy can be expressed as

$$F_R(\mathbf{n},T)=\tfrac{1}{2}(1-x)(F_{{\rm Er}(f)}+F_{{\rm Er}(g)}) +\tfrac{1}{2}x(F_{{\rm Dy}(f)}+F_{{\rm Dy}(g)}) . \tag{4}$$

The difference,

$$\Delta F_R(T)=F_R([100],T)-F_R([001],T) , \tag{5}$$

is the rare-earth ion's contribution to the stabilization energy of a magnetization alignment parallel to the c ([001]) axis, relative to a basal-plane (a axis or [100]) alignment. The total stabilization energy is given by

$$E_s(T)=\Delta F_R(T)+E_{\rm Fe}(T)+E_{\rm dip}(T) , \tag{6}$$

where $E_{\rm Fe}(T)$ is the anisotropy energy of the iron sublattice and $E_{\rm dip}(T)$ is the dipolar anisotropy of the R sublattice (both referred to one R ion). The former can be estimated from measurements of the anisotropy constant K_1 on $Y_2Fe_{14}B$;[7] at $T=0$ K it amounts to 0.8 MJ/m^3 or 6.6 K per R ion. The dipolar contribution was estimated by a lattice sum, yielding -1.5 K per R ion at $T=0$ K, and was scaled with a squared Brillouin function for its temperature dependence. Both contributions to $E_s(T)$ were thus represented, in the temperature range of interest ($T=0$ to 350 K), by an S-shaped curve ranging from 5.1 to 9.0 K per R ion.

The spin-reorientation temperature for a given concentration is then determined by the condition $E_s(T)=0$. We now discuss the choice of parameters in Eqs. (1)–(3).

The molecular field $H_{\rm mol}$ is related to the exchange field $H_{\rm ex}$ by $2\mu_B(g_J-1)\mathbf{J}\cdot\mathbf{H}_{\rm ex}=g_J\mu_B\mathbf{J}\cdot\mathbf{H}_{\rm mol}$. In $4f$-$3d$ intermetallic compounds, it can be usually assumed that f-f exchange is negligible compared to f-d exchange, so the exchange field acting on $4f$ ions should be essentially constant for a series of isostructural compounds; consequently, $H_{\rm mol}$ should scale with $(g_J-1)/g_J$. Measurements[7] based on the temperature dependence of the R sublattice magnetization in various $R_2Fe_{14}B$ alloys yielded the result

$$g_J\mu_B H_{\rm mol}(T=0\ {\rm K})/(g_J-1)=375\ {\rm K} ,$$

in good agreement with previous results for $Gd_2Fe_{14}B$ (Ref. 22) and for $Dy_2Fe_{14}B$ (Ref. 23). We thus take $g_J\mu_B H_{\rm mol}(0)=75$ K and 125 K for Er and Dy, respectively. Its temperature dependence was described by the equation

$$H_{\rm mol}(T)=H_{\rm mol}(0)[1-0.5(T/T_C)^2] ,$$

valid up to $T\simeq 0.8T_C$.[24] The concentration dependence of T_C (Table I) was also taken into account.

CEF parameters for the $R_2Fe_{14}B$ system have been evaluated by means of point-charge calculations by several authors.[15,25,26] Though useful in establishing general trends (e.g., the dominant role of second-order terms), such calculations are too uncertain to be quantitatively reliable. An experimental approach to second-order CEF parameters is provided by ^{155}Gd Mössbauer spectroscopy, via lattice electric-field-gradient (EFG) measurements. The B_2^0 and B_2^2 parameters are related to the lattice V_{zz} and η by[27]

$$B_2^0=-\frac{\alpha_J\langle r^2\rangle(1-\sigma_2)}{4(1-\gamma_\infty)}eV_{zz}^{\rm lat} , \qquad |B_2^2|=|B_2^0|\eta^{\rm lat} , \tag{7}$$

where α_J is the second-order Stevens coefficient,[17] $\langle r^2\rangle$ is a radial average over $4f$ electrons,[28] and σ_2 and γ_∞ are

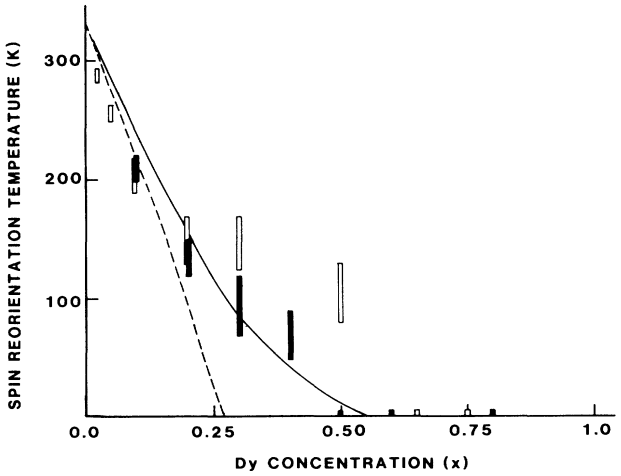

FIG. 2. Spin reorientation temperature as a function of x for $(Er_{1-x}Dy_x)_2Fe_{14}B$. Experimental data: this work (solid bars) and Ref. 14 (open bars). Calculated values: using second-order CEF terms only (dashed curve) and using second-, fourth-, and sixth-order CEF terms (solid curve).

electronic shielding parameters. Unfortunately, no well-established values for the lattice parameters are available. Theoretical and experimental estimates[29–31] for the heavier rare-earth metals range from -60 to -80 (γ_∞) and from 0.3 to 0.5 (σ_2). It has further been argued[32] that in metallic systems conduction electrons can strongly enhance the Sternheimer factor γ_∞; however, accepted values of the ratio $(1-\gamma_\infty)/(1-\sigma_2)$ range between 112 and 300.[31,33]

EFG parameters for the two Gd sites in $Gd_2Fe_{14}B$ have been determined by Bogé *et al.*[34] by means of ^{155}Gd Mössbauer spectroscopy. Their data can be used to estimate B_2^0 for Er. But, owing to the uncertainty on the conversion constant between the lattice quadrupole coupling constant and B_2^0, we have taken the proportionality constant as a free parameter; the latter was adjusted by setting the calculated T_r for $Er_2Fe_{14}B$ equal to the experimental value of 328 K.[10] B_2^2 was computed from B_2^0 with the asymmetry parameter obtained from the ^{155}Gd quadrupole interaction data.[34] The Dy parameters were obtained from the Er ones by scaling with the corresponding $\alpha_J\langle r^2\rangle$ factors,[17,28] i.e., $B_2^m(\mathrm{Dy}) = -2.73B_2^m(\mathrm{Er})$. The whole set of parameters is displayed in Table II. Notice that the B_2^0 values reported in Table II correspond to a ratio $(1-\gamma_\infty)/(1-\sigma_2)\simeq 240$.

It should be pointed out[35] that the presence of a 4_2 screw axis in the $R_2Fe_{14}B$ structure (space group $P4_2/mnm$) entails the subdivision of each of the $4f$ and $4g$ sites into two magnetically nonequivalent subsites, obtained from one another by a 90° rotation, and having B_2^2 values of opposite signs.

The calculated concentration dependence of T_r is shown in Fig. 2 (dashed curve). It is worth emphasizing that no adjustable parameters are involved at this stage. There is excellent agreement for small Dy concentrations ($x \lesssim 0.15$), or for not too low temperatures ($T_r > 160$ K). It thus appears that Hamiltonian (1), with CEF interactions limited to second-order terms, is a good approximation at moderately low temperatures.

Before proceeding to discuss the low-temperature region, we would like to comment on the apparent temperature range of the spin reorientation represented by error bars in Fig. 2. A possible explanation would be a T_r spread caused by sample inhomogeneity. Alternatively, a gradual spin reorientation can also be envisaged, the angle θ between magnetization and c axis being a continuous function of temperature.

Evidence favoring the second interpretation is provided by the behavior of the outermost positive-velocity line in the Mössbauer spectra, illustrated in Fig. 3. The sextet comprising this line has been assigned[15,36,37] to the $8j_2$ site,[20,21] and its isolated position results from both a large H_{eff} and a large quadrupole interaction. Due to the factor $(3\cos^2\theta - 1)$, the latter changes by a factor of $-\frac{1}{2}$ upon spin reorientation, shifting the j_2 line towards more negative velocities so that it becomes unresolved at low temperatures. Examining the spectra in Fig. 3, one can see the j_2 line gradually shift as T is lowered (the T_r range for this sample is from 50 to 90 K), implying a continuous θ variation with temperature. If inhomogeneity were preponderant, the resolved j_2 line would gradually lose intensity at its original position.

Our model, on the other hand, is consistent with a continuous process. The single-ion free energy can be calculated for any θ value [i.e., **n** in Eq. (3)], and the Fe-sublattice and R dipolar anisotropies can be reasonably assumed to vary as $\sin^2\theta$;[7,26] by minimizing the total anisotropy energy $E(\theta)$, one can calculate the equilibrium θ at any temperature. It turns out that, for every x, a temperature interval ΔT_r is found for which $E(\theta)$ has an absolute minimum at some intermediate angle. Examples are shown in Fig. 4. ΔT_r's of some tens of K are found for $x \neq 0$, while for $x = 0$, a much narrower transition region is obtained, exactly as found experimentally. The reason for this difference in behavior between ternary and pseudoternary alloys is, in our view, relatively trivial:

TABLE II. Single-ion Hamiltonian parameters used to calculate T_r vs x (dashed curve in Fig. 2).

Ion (site)	B_2^0 (K)[a]	B_2^2 (K)	$g_J\mu_B H_{\mathrm{mol}}$ (K)
Er ($4f$)	0.40	± 0.25	75
Er ($4g$)	0.38	± 0.75	75
Dy ($4f$)	-1.10	∓ 0.67	125
Dy ($4g$)	-1.02	∓ 2.00	125

[a]Referred to c axis.

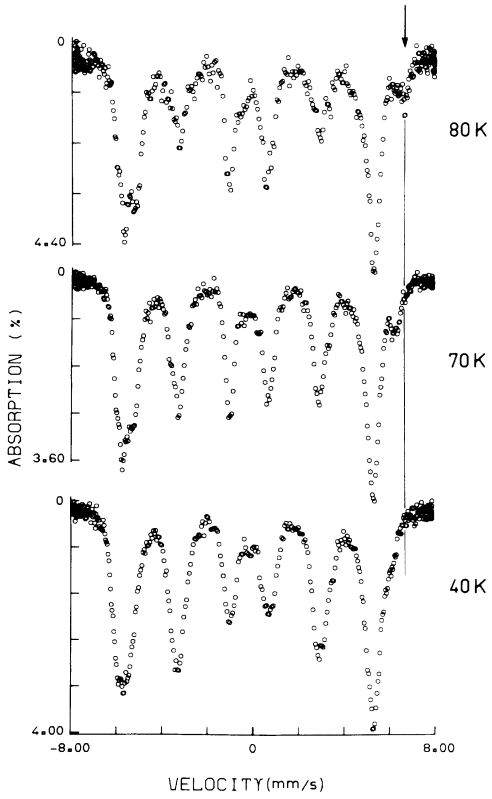

FIG. 3. Mössbauer spectra of magnetically aligned $(Er_{0.6}Dy_{0.4})_2Fe_{14}B$ at decreasing temperatures in the spin reorientation range. Notice the simultaneous gradual increase in $\Delta m = 0$ lines intensity and shift of the j_2 line (marked by arrow).

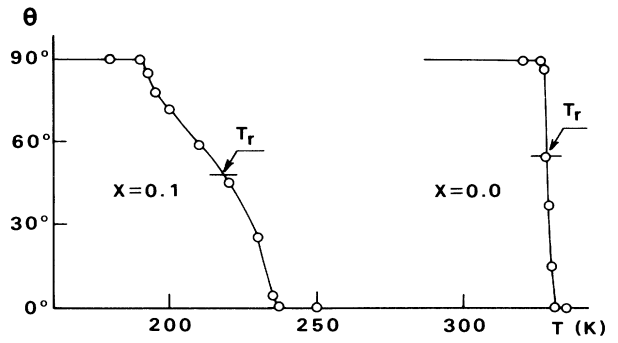

FIG. 4. Calculated equilibrium angle θ between magnetization and c axis as a function of temperature for $Er_2Fe_{14}B$ and $(Er_{0.9}Dy_{0.1})_2Fe_{14}B$. Calculated spin reorientation temperatures are indicated.

when the total $E(\theta)$ is a sum of three competing terms, each with its particular θ dependence, minima at intermediate angles are more likely to occur than when only two terms are competing. In this respect, the $(Er_{1-x}Gd_x)_2Fe_{14}B$ system is similar to $Er_2Fe_{14}B$, and accordingly, it exhibits rather sharp reorientations for all x.[13]

We now turn back to discussing the low-temperature data in Fig. 2. Our measurements suggest that basal-plane magnetization becomes unstable at $T=0$ K for a Dy concentration $x_c \simeq 0.5$; our model, on the other hand, predicts $x_c = 0.26$. The theoretical result is largely insensitive to the choice of B_2^0 and B_2^2 parameters, as the following arguments will demonstrate.

Consider the simplified Hamiltonian $\mathcal{H} = \mathcal{H}_{ex} + B_2^0 O_2^0$. At $T=0$ K, the single-ion stabilization energy $E_s(0)$ [cf. Eq. (5)] is simply the difference between the ground-state energies for exchange field perpendicular and parallel to the CEF axis. As was first noted by Greedan and Rao,[5] if exchange dominates ($g_J \mu_B H_{mol} \gg |B_2^0|$, as in our case), the stabilization energy (of either sign) is given approximately by $E_s(0) = -kB_2^0$, where k is a numerical constant. For $J = \frac{15}{2}$ ions such as Er and Dy, one finds $k \simeq 157$.

This result will be modified by inclusion of a $B_2^2 O_2^2$ term in the Hamiltonian. As already noted, however, in the $R_2Fe_{14}B$ structure B_2^2 values occur in pairs with opposite signs, and as a consequence the changes in $E_s(0)$ induced by this term are largely canceled out.

Thus, for a $(R_{1-x}R'_x)_2Fe_{14}B$ alloy, the stabilization energy of 0 K is given approximately by

$$E_{s(0)} = -kB_2^0(R)(1-x) - k'B_2^0(R')x + E_a \ , \tag{8}$$

where E_a is the anisotropy energy from other sources. If $B_2^0(R)$ and $B_2^0(R')$ have opposite signs, $E_s(0)$ will vanish for a finite $x = x_c$; neglecting E_a, one obtains an upper limit for x_c

$$x_c \lesssim \frac{1}{1 - k'|B_2^0(R')|/k|B_2^0(R)|} \ , \tag{9}$$

which depends only on purely atomic scaling factors. For $R = Er$ and $R' = Dy$, one gets $x_c \lesssim 0.27$, in agreement with the full calculation result. It is thus clear that the large discrepancy between theoretical and experimental x_c cannot be removed by any choice of second-order CEF parameters.

We therefore investigated the effect of higher-order CEF terms on x_c. Among all fourth-order and sixth-order terms, the dominant ones with respect to uniaxial anisotropy are $B_4^0 O_4^0$ and $B_6^0 O_6^0$, respectively. The ground-state energy of the Hamiltonian

$$\mathcal{H} = B_2^0 O_2^0 + B_4^0 O_4^0 + B_6^0 O_6^0 - g_J \mu_B H_{mol} \mathbf{J}\cdot\mathbf{n} \tag{10}$$

was calculated for $\mathbf{n}$ parallel and perpendicular to the c axis, their difference $E_s = E_\perp - E_\parallel$ being the stabilization energy for the ion in question (other anisotropy sources are not considered at this stage). B_2^0 was taken equal to 0.4 K and B_4^0, B_6^0 were varied. [In the following, all quoted CEF parameter values will refer to the Er ion; the corresponding Dy parameters are obtained by scaling with the factors[17,28] -2.73 (B_2^0), -1.57 (B_4^0), and 0.61 (B_6^0).]

Figure 4 displays some calculated stabilization energies for both ions; we chose $B_4^0 < 0$ and $B_6^0 > 0$, in accordance with point-charge calculations.[25] The kink in most E_s versus B_4^0 curves corresponds to a level crossing between different $|J_z\rangle$ ground states ($|\frac{15}{2}\rangle \rightarrow |\frac{13}{2}\rangle$ for Dy, $|\frac{13}{2}\rangle \rightarrow |\frac{15}{2}\rangle$ for Er) in the parallel field case.

Our experimental $x_c \simeq 0.5$ implies that one should have $E_s(Dy)/|E_s(Er)| \simeq 1$. The $B_6^0 = 0$ curves in Fig. 5 show that this ratio is never approached under the influence of B_4^0 alone. $B_4^2 O_4^2$ and $B_4^4 O_4^4$ terms were tentatively included, with no significant effect. All terms in (10) are indeed needed to make the two E_s approach each other in the required way, the most favorable parameters combination being close to $B_4^0 = -3\times10^{-3}$ K and $B_6^0 = 5\times10^{-5}$ K. Other combinations with $B_4^0 > 0$ and/or $B_6^0 < 0$ were tried without success.

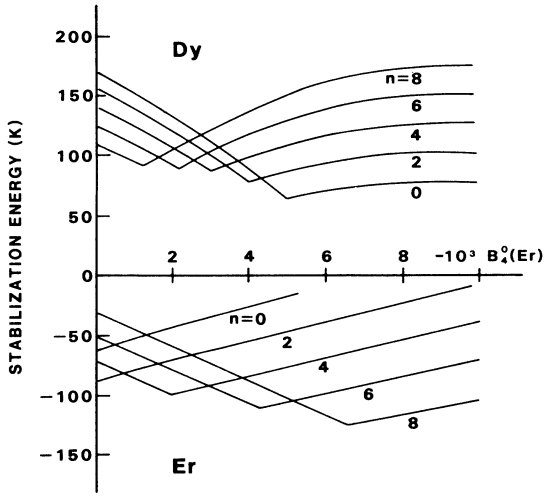

FIG. 5. Stabilization energy of c-axis magnetization at $T=0$ K, calculated from Hamiltonian (10), for Dy (positive values) and Er (negative values). Each curve represents $E_s(0)$ as a function of B_4^0(Er), with fixed B_2^0(Er) = 0.4 K and B_6^0(Er) = $n\times10^{-5}$ K with n as indicated. Corresponding CEF parameters for Dy are obtained by scaling (see text).

TABLE III. Single-ion Hamiltonian CEF parameters used to calculate T_r vs x (solid curve in Fig. 2). Exchange parameters are the same as in Table II.

Ion (site)	B_2^0 (K)	B_2^2 (K)	B_4^0 (K)	B_6^0 (K)
Er ($4f$)	0.36	± 0.22	-3.0×10^{-3}	5.0×10^{-5}
Er ($4g$)	0.34	± 0.66	-3.0×10^{-3}	5.0×10^{-5}
Dy ($4f$)	-0.98	∓ 0.60	4.7×10^{-3}	3.1×10^{-5}
Dy ($4g$)	-0.91	∓ 1.80	4.7×10^{-3}	3.1×10^{-5}

Finally, we studied the influence of B_4^0 and B_6^0 on the spin reorientation at finite temperatures. We calculated T_r as a function of x, through Eq. (6), starting from the Hamiltonian (1)–(3) augmented with fourth- and sixth-order axial CEF terms. We chose $B_4^0 = -3\times10^{-3}$ K and $B_6^0 = 5\times10^{-5}$ K without distinguishing between $4f$ and $4g$ sites; the original B_2^0 and B_2^2 values were scaled down by about 10% in order to preserve agreement for $x=0$. The new set of parameters is listed in Table III. Results are displayed in Fig. 2 (solid curve). It should be noted that the quantity T_r can be associated with the reorientation process in an experimentally meaningful way, even if it does not represent a sharp transition temperature. It can be appreciated from Fig. 2 that calculated $T_r(x)$ satisfactorily reproduces the general trends of our data. The effect of higher-order terms is preponderant at low temperatures and decreases rapidly with increasing temperature, as expected. It should be emphasized that inclusion of the sixth-order term was found to be essential at low temperatures. Its role in the present context can probably be traced back to the fact that the sixth-order Stevens coefficient γ_J has the same sign for Er and Dy, contrarily to α_J and β_J.

V. SUMMARY AND CONCLUSIONS

All $R_2Fe_{14}B$ alloys in which R has a positive Stevens coefficient α_J exhibit easy-plane magnetization at low temperatures. At higher temperatures, the Fe sublattice uniaxial anisotropy may become dominant, leading to a magnetization reorientation from the basal plane to the c axis. Since the average R anisotropy can be varied continuously by mixing different rare earths, spin reorientation studies as a function of composition are worthwhile as a means of improving our understanding of crystal field effects in these alloys.

We investigated the spin reorientation in $(Er_{1-x}Dy_x)_2Fe_{14}B$ alloys, by means of ^{57}Fe Mössbauer spectroscopy on magnetically aligned samples. Data were compared to predictions of a model incorporating single-ion CEF interactions, exchange interactions in the molecular-field approximation, and Fe sublattice and R dipolar anisotropy energies.

Er substitution by Dy reduces the spin reorientation temperature at a rate which, for small x, is in quantitative agreement with model predictions based on second-order CEF terms only. In addition, our measurements reveal that spin reorientations in the pseudoternary alloys occurs gradually over temperature intervals of some tens of K. This too is in agreement with model calculations, which exhibit free-energy minima at intermediate angles between the c axis and the basal plane for certain temperature ranges.

At higher Dy concentration, on the other hand, spin reorientation temperatures strongly depart from calculated ones, basal-plane magnetization remaining stable at 4.2 K up to $x \simeq 0.5$. This apparent reduction of the Dy ability to overcome the Er basal anisotropy can be accounted for by taking both fourth- and sixth-order CEF into consideration. Such terms are generally expected to be important at low temperatures; thus, fourth order terms are needed to describe the spin canting below 150 K in $Nd_2Fe_{14}B$. The present work, however, provides the first example of the necessity of using sixth-order CEF terms to fit experimental data on $R_2Fe_{14}B$ alloys.

ACKNOWLEDGMENTS

We are grateful to A. Bonnenfant and R. Poinsot for technical assistance. H.R.R. acknowledges financial support from Fundação de Amparo e Pesquisa do Estado de São Paulo (Brazil). This work was partially supported by the Commission of European Communities through the CEAM program.

*On leave from Instituto de Física, Universidade de São Paulo, São Paulo, Brazil.

[1]For a recent review see K. H. J. Buschow, Mater. Sci. Rep. **1**, 1 (1986).
[2]J. J. Croat, J. F. Herbst, R. W. Lee, and F. E. Pinkerton, J. Appl. Phys. **55**, 2078 (1984).
[3]M. Sagawa, S. Fujimura, M. Togawa, H. Yamamoto, and Y. Matsuura, J. Appl. Phys. **55**, 2083 (1984).
[4]S. Sinnema, R. J. Radwanski, J. J. M. Franse, D. B. de Mooij, and K. H. J. Buschow, J. Magn. Magn. Mater. **44**, 333 (1984).
[5]J. E. Greedan and V. U. S. Rao, J. Solid State Chem. **6**, 387 (1973).
[6]C. Abache and H. Oesterreicher, J. Appl. Phys. **57**, 4112 (1985).
[7]S. Hirosawa, Y. Matsuura, H. Yamamoto, S. Fujimura, and M. Sagawa, J. Appl. Phys. **59**, 873 (1986).
[8]E. B. Boltich and W. E. Wallace, Solid State Commun. **55**, 529 (1985).

[9]S. Hirosawa and M. Sagawa, Solid State Commun. **54**, 335 (1985).
[10]A. Vasquez, J. M. Friedt, J. P. Sanchez, Ph. L'Héritier, and R. Fruchart, Solid State Commun. **55**, 783 (1985).
[11]D. C. Price, R. K. Day, and J. B. Dunlop, J. Appl. Phys. **59**, 3585 (1986).
[12]P. Burlet, J. M. D. Coey, J. P. Gavigan, D. Givord, and C. Meyer, Solid State Commun. **60**, 723 (1986).
[13]A. Vasquez and J. P. Sanchez, J. Less-Common Metals **127**, 71 (1987).
[14]D. Niarchos and A. Simopoulos, Solid State Commun. **59**, 669 (1986).
[15]J. M. Friedt, A. Vasquez, J. P. Sanchez, Ph. L'Héritier, and R. Fruchart, J. Phys. F **16**, 651 (1986).
[16]H. R. Rechenberg, A. Paduan-Filho, F. P. Missell, P. Deppe, and M. Rosenberg, Solid State Commun. **59**, 541 (1986).
[17]U. Atzmony, M. P. Dariel, E. R. Bauminger, D. Lebenbaum, I. Nowik, and S. Ofer, Phys. Rev. B **7**, 4220 (1973).
[18]M. T. Hutchings, Solid State Phys. **16**, 227 (1966).
[19]D. Givord, H. S. Li, and J. M. Moreau, Solid State Commun. **50**, 497 (1984).
[20]J. F. Herbst, J. J. Croat, F. E. Pinkerton, and W. B. Yelon, Phys. Rev. B **29**, 4176 (1984).
[21]C. B. Shoemaker, D. P. Shoemaker, and R. Fruchart, Acta Crystallogr. Sect. C **40**, 1665 (1984).
[22]M. Bogé, J. M. D. Coey, G. Czjzek, D. Givord, C. Jeandey, H. S. Li, and J. L. Oddou, Solid State Commun. **55**, 295 (1985).
[23]Y. Berthier, M. Bogé, G. Czjzek, D. Givord, C. Jeandey, H. S. Li, and J. L. Oddou, J. Magn. Magn. Mater. **54-57**, 589 (1986).
[24]P. C. M. Gubbens, A. M. van der Kraan, and K. H. J. Buschow, Phys. Status Solidi B **130**, 575 (1985).
[25]J. M. Cadogan and J. M. D. Coey, Phys. Rev. B **30**, 7326 (1984).
[26]D. Givord, H. S. Li, and R. Perrier de la Bâthie, Solid State Commun. **51**, 857 (1984).
[27]S. Ofer, I. Nowik, and S. G. Cohen, in *Chemical Applications of Mössbauer Spectroscopy,* edited by V. I. Goldanskii and R. H. Herber (Academic, New York, 1968), p. 428.
[28]A. J. Freeman and R. E. Watson, Phys. Rev. **127**, 2058 (1962).
[29]J. Blok and D. A. Shirley, Phys. Rev. **143**, 278 (1966).
[30]R. P. Gupta, and S. K. Sen, Phys. Rev. A **7**, 850 (1973).
[31]J. M. Friedt, G. K. Shenoy, and B. D. Dunlap, J. Phys. (Paris) Colloq. **40**, C2-243 (1978).
[32]J. Pelzl, Z. Phys. **251**, 13 (1972).
[33]H. H. Wickman and I. Nowik, Phys. Rev. **142**, 115 (1966).
[34]M. Bogé, G. Czjzek, D. Givord, C. Jeandey, H. S. Li, and J. L. Oddou, J. Phys. F **16**, L67 (1986).
[35]M. Yamada, Y. Yamaguchi, H. Kato, H. Yamamoto, Y. Nakagawa, S. Hirosawa, and M. Sagawa, Solid State Commun. **56**, 663 (1985).
[36]H. Onodera, Y. Yamaguchi, H. Yamamoto, M. Sagawa, Y. Matsuura, and H. Yamamoto, J. Magn. Magn. Mater. **46**, 151 (1984).
[37]H. M. van Noort, D. B. de Mooij, and K. H. J. Buschow, J. Appl. Phys. **57**, 5414 (1985).